Supplemental material

Different mechanisms of GIP and GLP-1 action explain their different therapeutic efficacy in type 2 diabetes

E. Grespan, T. Giorgino, A. Natali, E. Ferrannini and A. Mari

1 Model and simulation details

The model used to study the effects of GIP and GLP-1 is an expansion of the model previously developed to describe the response to intravenous glucose (Grespan et al., 2018).

1.1 Model equations

1.1.1 Immediately releasable pool dynamics equations

The core of the model, represented in Figure 1B of the main text, is the immediately releasable pool (IRP), which accounts for the insulin granules that undergo rapid exocytosis when intracellular calcium increases (triggering pathway). Over a longer time, insulin secretion is sustained by refilling of the IRP (amplifying pathway). Refilling is controlled by both calcium and glucose (through the refilling function). Calcium concentration is an input to the model and, along with glucose, is required to calculate insulin secretion. IRP dynamics are represented by the equation:

$$\frac{dQ}{dt} = -k(t)Q(t) + r(t) \tag{S.1}$$

where $Q(t)$ is the insulin mass in the IRP (measurements units depend on the experimental data, e.g., pmol per m^2 of estimated surface area), $k(t)$ is the calcium-controlled exocytosis rate constant (min^{-1}) and $r(t)$ is the refilling rate, dependent on both calcium and glucose (units are also experiment-specific, e.g., pmol min^{-1} m^{-2}).
The equations for k(t) and r(t) are:

$$k(t) = \partial_k\{f_k(C(t))\} \tag{S.2}$$

$$r(t) = \partial_r\{f_r(C(t), G(t))\} \tag{S.3}$$

To describe the dependence of $k(t)$ and $r(t)$ on calcium ($C(t)$, nmol/L) and glucose ($G(t)$, mmol/L), we use two functions, respectively $f_k(C(t))$ and $f_r(C(t), G(t))$, that are described in Section 1.1.2. The model assumes that a delay occurs between a change in glucose and calcium concentrations and the corresponding changes in $k(t)$ and $r(t)$. The delay is a combination of a time-shift and a first-order delay, and is represented in compact form with the operator $\partial\{\cdot\}$, where the subscript of $\partial\{\cdot\}$ indicates whether the delay refers to exocytosis or refilling. The delay functions are described in Section 1.1.3.
The instantaneous insulin secretion rate $S(t)$ (units are experiment-dependent, e.g., pmol $min^{-1}m^{-2}$) is:

$$S(t) = k(t)Q(t) \tag{S.4}$$

Equations (S.1)-(S.4), with initial steady-state conditions, provide the complete description of the model; insulin secretion can be predicted when both glucose and calcium are known.

1.1.2 Exocytosis and refilling functions

Both the exocytosis and the refilling functions $f_k(C)$ and $f_r(C, G)$ are based on the function of Mari et al. (Mari et al., 2002):

$$\begin{aligned} &h(C;\rho,\gamma,\sigma_1,\sigma_2) = \\ &\sigma_1 C - \frac{1}{\tanh(\gamma\rho)+1}(\sigma_1-\sigma_2)\times \\ &\quad\times\left(C\tanh(\gamma\rho) - \frac{1}{\rho}\left(\log(\cosh(\gamma\rho)) - \log(\cosh(\rho(\gamma - C(t))))\right)\right) \end{aligned} \tag{S.5}$$

The function is represented in Figure S1. The parameter γ divides the C axis ($C \geq 0$) in two regions in which $h(C)$ is a quasi-linear function with low sensitivity σ_1 (left to γ) or high sensitivity σ_2 (right to γ). The parameter ρ influences the curvature around γ. The function was obtained analytically as the integral of the hyperbolic tangent function, shifted and scaled to satisfy the above requirements and, additionally, $h(0) = 0$ (Mari et al., 2002).

The exocytosis function is simply:

$$f_k(C;p_1,p_2,p_3,p_4) = h(C;p_1,p_2,p_3,p_4) \tag{S.6}$$

The parameters ρ, γ, σ_1 and σ_2 for $f_k(C)$ are thus p_1 to p_4. The refilling function is:

$$\begin{aligned} f_r(C,G;p_5,p_6,p_7,p_8,p_9,p_{10},p_{11}) = \\ p_5 + h\big(C;p_6,p_7,p_8 w(G,p_9,p_{10},p_{11}),w(G,p_9,p_{10},p_{11})\big) \end{aligned} \tag{S.7}$$

where

$$w(G;p_9,p_{10},p_{11}) = p_9 \frac{1}{2}\left[1+\tanh\left(p_{10}(G-p_{11})\right)\right] \tag{S.8}$$

In the refilling function, the sensitivities for C, σ_1 and σ_2, are modulated by glucose concentration G via the sigmoidal function $w(G)$. In addition, the ratio of the sensitivities is the constant $\sigma_1/\sigma_2 = p_8$ and $f_r(0,G) = p_5$.

1.1.3 Delay

The delay with which calcium and glucose exert their actions on exocytosis and refilling is a combination of a time shift τ and a first-order delay with time constant $1/\alpha$. This composite delay is indicated with the operator $\partial(\cdot)$; $y(t) = \partial(x(t))$ is obtained by the following delay differential equation:

$$\frac{dy(t)}{dt} = \alpha(x(t-\tau) - y(t)) \tag{S.9}$$

For exocytosis (∂_k), the parameters are $p_{12} = \tau$ and $p_{13} = \alpha$; for the refilling (∂_r), $p_{14} = \tau$ and $p_{15} = \alpha$.It should be noted that the delay has a different physiological interpretation for the calcium effect on $k(t)$ and for the refilling. For $k(t)$, the role of the time-shift is to accommodate for possibly imprecise alignment of the calcium and secretion data; the potential delayed effect of calcium on $k(t)$ is accounted by the first-order delay component. Thus, ∂_k has a minor role. For $r(t)$, the delay is an essential component of the description, as a delayed rise of the refilling is crucial to explain typical features of insulin secretion.

1.1.4 Glucose-induced potentiation

The delay of the refilling function described in Equation S.9 accounts for the gradual increase of insulin secretion after constant hyperglycemic stimulus. However, when the increase over time was not sufficient to reproduce a strong rising second-phase secretion elicited by hyperglycemic clamps, we introduced a time-dependent factor (K_{glu}) that multiplies the slope above the threshold of the refilling function f_r, *i.e.*, the last argument of the function h in Equation S.7. K_{glu} is 1 at baseline and progressively increases during the glucose stimulus to a value at the end of the experiment that depends on the specific study, which in our simulations ranges between 1.3 to 2.8. Results on the K_{glu} increase are reported in the supplementary figures below.

1.1.5 Glucose-calcium relationship

The calcium response to a glucose stimulus is obtained as a sum of a static function of glucose concentration, $C_s(G)$, and a dynamic component, $C_d(t)$ (Figure S2):

$$C(t) = C_s(G(t)) + C_d(t) \tag{S.10}$$

In the sigmoidal static function

$$C_s(G) = p_{16}\frac{1}{2}\left[1+\tanh\left(p_{17}(G-p_{18})\right)\right] \tag{S.11}$$

the parameters are derived from the glucose-calcium relationship reported in Henquin et al. (Henquin et al., 2006).

The dynamic component $C_d(t)$ is obtained from a simple zero-gain linear system (with bi-dimensional state vector z) that generates a peak when glucose concentration is abruptly raised and a nonlinear function of glucose concentration that modulates the peak:

$$\frac{dz(t)}{dt} = \begin{bmatrix} -p_{19} & 0 \\ 0 & -p_{20} \end{bmatrix} z(t) + \begin{bmatrix} p_{19} \\ p_{20} \end{bmatrix} G(t) \qquad \text{with} \qquad z(0) = \begin{bmatrix} G(0) \\ G(0) \end{bmatrix} \tag{S.12}$$

$$C_d(t) = \max\left(0, \begin{bmatrix} 1 & -1 \end{bmatrix} z(t)\right) \left[\left(p_{21} - p_{22} \tanh(p_{23}(G(t) - p_{24})\right)\right] \tag{S.13}$$

1.1.6 Incretin effect on calcium

We assume that incretin hormones produce a transient increase in calcium. The peak increase varies in the different studies between 15 and 80 nmol/L and the duration of the peak varies between 15 and 30 minutes after the start of the incretin stimulus. In study B4, where a bolus of GIP was injected, the calcium peak is much higher (150 nmol/L in response to the low dose and 250 nmol/L in response to the high dose bolus) and it lasts 8 minutes. We assume that the effect of incretins is additive to that of glucose; therefore:

$$C_{total}(t) = C(t) + C_{incr}(t) \tag{S.14}$$

where $C(t)$ is the glucose-stimulated cytosolic calcium obtained from Equation S.10 and $C_{incr}(t)$ is the incretin-mediated transient increase in calcium. $C_{total}(t)$ is used in Equations S.5 - S.9 to reproduce the studies with incretin stimulation. $C_{incr}(t)$ was obtained in the various studies empirically, by fitting the model to the insulin secretion data. The mean $C_{incr}(t)$ in the various studies is reported in Table S3.

1.1.7 Incretin effect on refilling

We hypothesize that incretins increase the refilling function through a time-dependent factor K_{incr}; we assume that $K_{incr} = 1$ in the absence of incretin stimulation, while $K_{incr} > 1$ with incretin stimulation. The factor K_{incr} multiplies the slope above the threshold of the refilling function $f_r(C,G)$, i.e., the last argument of the function h in Equation S.7. When also glucose-induced potentiation (K_{glu}) is required, the slope above the threshold of the refilling function is multiplied by both K_{incr} and K_{glu}.

1.1.8 Calculation of the incretin effect on refilling from incretin hormones concentrations

The analysis of the mean K_{incr} values empirically calculated in the various studies versus the mean GIP or GLP-1 concentrations allowed us to define K_{incr}-hormone concentration relationships for GIP and GLP-1 (reported in Figure 5 of the main text). The equation describing the relationship between total GLP-1 concentration and the corresponding K_{incr} is:

$$K_{incrGLP1}(x) = \begin{cases} 1, & \text{if } x \leq \lambda_0. \\ 1 + \lambda(x - \lambda_0), & \text{if } x > \lambda_0. \end{cases} \tag{S.15}$$

where x is the measured GLP-1 concentration, λ_0 is a GLP-1 concentration threshold, below which it is assumed that GLP-1 does not affect the secretory response. In the curves reported in Figure 5 of the main text (light green lines), λ_0 was calculated as the mean value of the basal GLP-1 concentration of all studies; λ is the slope of the curve above λ_0 and was calculated empirically to fit the experimental data.
The relationship between total GIP concentration and the corresponding K_{incr} is given by the function:

$$K_{incrGIP}(x) = \begin{cases} 1, & \text{if } x \leq \eta_0. \\ 1 + \dfrac{K_{max}}{1 - \dfrac{1}{1 + exp(\theta\mu)}} \left(\dfrac{1}{1 + \exp(-\theta(x - \eta_0 - \mu))} - \dfrac{1}{1 + \exp(\theta\mu)} \right), & \text{if } x > \eta_0. \end{cases} \tag{S.16}$$

where x is the measured GIP concentration, $1+K_{max}$ is the function maximum value, θ determines the steepness of the curve transition from 1 to $1+K_{max}$, and μ influences the x-value at which the function value is $1+K_{max}/2$. η_0 is a GIP concentration threshold, below which it is assumed that GIP does not affect the secretory response. In the curves reported in Figure 5 of the main text (dark green lines) η_0 was calculated as the mean value of the basal GIP concentration of all studies. θ was calculated empirically to fit the data. The study of Nauck et al. (M. A. Nauck et al., 1993) reported in Figure 6 of the main text and in Figure S10 is based on the relationships described by Equations S.15 and S.16.
In the OGTT and in the test with simultaneous infusion of GIP and GLP-1, the effects of GIP and GLP-1 were assumed to be additive and the total K_{incr} was calculated by the equation:

$$K_{incr}(x) = K_{incrGLP1}(x) + K_{incrGIP}(x) - 1 \tag{S.17}$$

The parameters used to calculate $K_{incrGIP}(x)$ and $K_{incrGLP1}(x)$ in Figure 5 of the main text and in Figure S10B are reported in Table S2.

1.2 Model code

An implementation of the model in the Matlab and Simulink languages is provided at the address `https://github.com/CNR-IN-MatMod/IncretinModel2019`.

2 Potentiating effects of GIP in nondiabetic subjects: a systematic review

In our modeling analysis of the effects of GIP on insulin secretion, we have included the studies that we thought were more relevant, particularly for the historical value, the detailed analysis and the wide range of GIP doses. To further support our finding of a saturative effect of GIP in nondiabetic subjects, we performed a more systematic literature search. To capture the studies employing hyperglycemic clamps with GIP infusion on human subjects we performed a search in PubMed on October 31, 2019. We used the search string "(hyperglycaemic OR hyperglycemic OR hyperglycaemia OR hyperglycemia) AND (clamp OR clamps OR clamping OR clamped) AND (insulinotropic polypeptide OR GIP OR gastric inhibitory polypeptide) AND Humans[MeSH]". We repeated the search omitting the "Humans[MeSH]"criterion to include additional publications in 2019 lacking the MeSH tag. The search yielded 90 publications.
We then reviewed the results and selected the studies satisfying the following inclusion criteria:

- Studies actually performed in human subjects
- Studies including subjects without T2D
- Studies with GIP infusions
- Studies actually using a standardized hyperglycemic clamp
- Studies including a separate test with saline infusion or a clamp period without GIP infusion
- Studies not included in the main analysis (Studies B)

Exclusion criteria where:

- Publications without original data, i.e. secondary studies using data included in other publications considered in the present analysis
- Studies using a GIP receptor inhibitor as a control condition
- Studies using somatostatin or diazoxide
- Studies with GIP infused in combination with GLP-1
- Studies with appropriate protocol but without C-peptide or insulin
- Studies with hyperglycemic-hyperinsulinemic clamp without C-peptide

Fifteen studies satisfied the selection criteria. To these studies, we added two additional known publications satisfying the criteria but not retrieved via the PubMed search (Elahi et al., 1994 and Vilsbøll et al., 2003). The complete results of the review are available at the address `https://github.com/CNR-IN-MatMod/IncretinModel2019`.
The seventeen included studies employed different protocols. In particular, most studies employed a control test with the hyperglycemic clamp performed with saline infusion. Some studies did not use a separate control test but administered GIP after a control period of the hyperglycemic clamp without GIP infusion. The accuracy of the estimated potentiating effect of GIP on ISR is reduced in these studies, as ISR may increase considerably over time without

GIP stimulation (e.g. Figure S5). One study, designed for assessing the effects of GIP on fat metabolism, employed a hyperglycemic-hyperinsulinemic clamp, i.e., a hyperglycemic clamp with exogenous insulin infusion to reach standardized insulin levels.
Most studies reported ISR calculated from C-peptide or C-peptide concentration. A few studies reported only insulin concentration. The estimated potentiating effect of GIP on ISR may be biased when evaluated using insulin concentration, as insulin clearance may differ in the two study conditions (e.g. Rudovich et al., 2004).
To assess the potentiating effect of GIP on ISR, we have first evaluated ISR under control and GIP-stimulated conditions from the results of the publications. These values were obtained from the reported ISR, if available, or from C-peptide or insulin concentrations. Data were reconstructed from the figures if necessary. ISR, C-peptide or insulin concentration are reported as mean values during the appropriate experimental periods. The potentiating effect of GIP on ISR was calculated as the fold increase in insulin secretion (or C-peptide or insulin) with GIP infusion compared to saline infusion or to the clamp control period. The results are reported in Table S4 and Figure S13. Additional details of the calculations are reported in the table legend, if necessary.

3 Supplementary tables

				NGT[a]								T2D[b]							
Par.	**Eq.**	**Description**	**Unit**	**Study A1**	**Study B1**	**Study B2**	**Study B3**	**Study B4**	**Study B5**	**Study C1**	**Study D1**	**Study A2**	**Study B1**	**Study B2**	**Study B3**	**Study B4**	**Study B5**	**Study C1**	**Study D2**
p1		ρ for exocytosis	$(nmol/L)^{-1}$	1.5	1.5	1.5	1.5	1.5	1.5	1.5	1.5	1.5	1.5	1.5	1.5	1.5	1.5	1.5	1.5
p2		γ for exocytosis	nmol/L	95	95	95	98	105	96.9	95	105	95	95	95	98	105	96.9	95	105
p3	S.1	σ_1 for exocytosis	$(nmol/L)^{-1}\times min^{-1}$	2.00×10^{-4}	2.00×10^{-4}	2.00×10^{-4}	2.00×10^{-4}	2.00×10^{-4}	2.00×10^{-4}	2.00×10^{-4}	2.00×10^{-4}	2.00×10^{-4}	2.00×10^{-4}	2.00×10^{-4}	2.00×10^{-4}	2.00×10^{-4}	2.00×10^{-4}	2.00×10^{-4}	2.00×10^{-4}
p4		σ_2 for exocytosis	$(nmol/L)^{-1}\times min^{-1}$	2.90×10^{-3}	2.90×10^{-3}	2.90×10^{-3}	2.90×10^{-3}	2.90×10^{-3}	2.90×10^{-3}	2.90×10^{-3}	2.90×10^{-3}	2.90×10^{-3}	2.90×10^{-3}	2.90×10^{-3}	2.90×10^{-3}	2.90×10^{-3}	2.90×10^{-3}	2.90×10^{-3}	2.90×10^{-3}
p5		$f_r(0, G)$	[S]	134	241	144	288	104.5	113.46	134	108	34.8	117.9	174	213	6.7	73.75	134	155.25
p6		ρ for refilling	$(nmol/L)^{-1}$	1.5	1.5	1.5	1.5	1.5	1.5	1.5	1.5	1.5	1.5	1.5	1.5	1.5	1.5	1.5	1.5
p7		γ for refilling	nmol/L	102	102	102	109	102	102	102	102	90	102	102	109	102	102	102	102
p8	S.3	σ_1/σ_2 for refilling	--	0	0	0	0	0	0	0	0	0	0	0	0	0	0	0	0
p9	S.4	σ_2 for refilling at $G\rightarrow\infty$	$[S]\times(nmol/L)^{-1}$	17.83	10.16	11.23	10.51	16.94	9.81	11.73	8.66	5.26	9.54	2.66	4.2	6.24	4.26	3.56	4.91
p10		w slope at G = p11	$(mmol/L)^{-1}$	0.0669	0.0669	0.0555	0.1302	0.0669	0.0555	0.0669	0.052	0.0669	0.0669	0.0555	0.1302	0.0669	0.0555	0.0669	0.052
p11		w glucose offset	mmol/L	13.18	13.18	18.3	17.02	13.18	18.31	13.18	7.8	13.18	13.18	18.31	17.02	13.18	18.31	13.18	7.8
p12	S.5	τ for exocytosis	min	0	0	0	0	0	0	0	0	0	0	0	0	0	0	0	0
p13	∂_k	α for exocytosis	min^{-1}	2.1	2.1	2.1	2.04	2.1	2.1	2.1	2.1	2.1	2.1	2.1	2.04	2.1	2.1	2.1	2.1
p14	S.5	τ for refilling	min	4.28×10^{-5}	4.28×10^{-5}	4.28×10^{-5}	4.28×10^{-5}	4.28×10^{-5}	4.28×10^{-5}	4.28×10^{-5}	4.28×10^{-5}	4.28×10^{-5}	4.28×10^{-5}	4.28×10^{-5}	4.28×10^{-5}	4.28×10^{-5}	4.28×10^{-5}	4.28×10^{-5}	4.28×10^{-5}
p15	∂r	α for refilling	min^{-1}	0.095	0.095	0.095	0.312	0.266	0.0665	0.095	0.095	0.095	0.095	0.095	0.624	0.266	0.095	0.095	0.095
p16		Cs max	nmol/L	256	256	256	256	256	256	256	256	256	256	256	256	256	256	256	256
p17	S.7	Cs slope at G = p18	$(mmol/L)^{-1}$	0.148	0.148	0.148	0.148	0.148	0.148	0.148	0.148	0.148	0.148	0.148	0.148	0.148	0.148	0.148	0.148
p18		Cs glucose offset	mmol/L	6.8	6.8	6.8	6.8	6.8	6.8	6.8	6.8	6.8	6.8	6.8	6.8	6.8	6.8	6.8	6.8
p19		Cd peak shape	min^{-1}	2	2	2	2	2	2	2	2	2	2	2	2	2	2	2	2
p20		Cd peak shape	min^{-1}	1.5	1.5	1.5	1.5	1.5	1.5	1.5	1.5	1.5	1.5	1.5	1.5	1.5	1.5	1.5	1.5
p21	S.8	Cd peak amplitude	nmol/L	10	10	10	10	10	10	10	10	10	10	10	10	10	10	10	10
p22	S.9	Cd peak amplitude	nmol/L	0.5	0.5	0.5	0.5	0.5	0.5	0.5	0.5	0.5	0.5	0.5	0.5	0.5	0.5	0.5	0.5
p23		Cd slope at G = p24	$(mmol/L)^{-1}$	15	15	15	15	15	15	15	15	15	15	15	15	15	15	15	15
p24		Cd glucose offset	mmol/L	120	120	120	120	120	120	120	120	120	120	120	120	120	120	120	120
K_{glu}	-	Max K_{glu} value	-	-	1.5	2.8	2.8	1.2	1.4	-	-	2.2	1.1	1.4	1.4	-	1.2	-	-

[a] Normal glucose tolerance; [b] Type 2 diabetes.

Table S1: Model parameters. [S] indicates the unit of insulin secretion, which is experiment-dependent.

Parameters	Equations	Reference curves		Study D1	Study D2
		NGT[a]	T2D[b]	NGT	T2D
λ_0 (pmol/L)	S.11	16	16	11	16
λ (pmol/L) $^{-1}$		0.08	0.056	0.19	0.001
η_0 (pmol/L)	S.12	24	24	15.5	24
K_{max}		1.1	0.6	1.1	0
θ (pmol/L) $^{-1}$		0.06	0.06	0.06	0.06
μ (pmol/L)		25	25	25	25

[a] Normal glucose tolerance; [b] Type 2 diabetes.

Table S2: Parameters for the calculation of the hormone concentrations-K_{incr} relationships described in Equations S.15 – S.17.

	GIP			GLP-1		
Study	Dose	NGT[a]	T2D[b]	Dose	NGT	T2D
A1	2	23	-	0.75	25	-
A2	4	-	31	1.2	-	31
B1	0.8	31	22	0.4	37	37
	2.4	32	32	1.2	39	39
B2	1.5	46	46	0.5	46	46
B3	4	53	53	1	-	53
	16	-	53	-	-	-
B4	1	88	73	-	-	-
	4	173	100	-	-	-
B5	8	46	46	1	46	46
C1	-	-	-	0.5	10	8
	-	-	-	1	17	13
	-	-	-	2	23	19
D1	1	12	-	0.3	12	-
D2	4	-	49	0.6	-	97

[a] Normal glucose tolerance; [b] Type 2 diabetes.

Table S3: Mean (as AUC/time) transient calcium increase above the glucose-stimulated levels. GIP and GLP-1 doses are in pmol·kg^{-1}·min^{-1}. In Study B4, GIP infusions were accompanied by a priming dose of 20 or 80 pmol/kg. In Study A1, the calcium profile is univocally determined by the data and independent of K_{incr}. In Studies B1-B5 the calcium profile is defined by the data, once K_{incr} is fixed. In the other studies, the calcium increase due to incretins was less clearly determinable. In these studies, we simulated a calcium rise that reproduced the data appropriately and was consistent with the other studies. The estimated effect on transient calcium increase was similar for GIP and GLP-1 and was preserved in T2D compared to NGT.

Reference	Protocol	Group	GIP dose	CTR ISR	GIP ISR	CTR INS	GIP INS	POT ISR	POT INS
Asmar, M. 2010	HI-HGC		1.5	638	1180			1.85	
Christensen, M. 2011 (a)	HGC-Saline		2	7.3*	16.4	214	800.5	2.25	3.74
Dirksen, C. 2013	HGC-Saline		1.5	7*	10.45				
Elahi, D. 1994	HGC-Saline		1			235	351		1.49
			2			235	936		3.98
			4			235	1165		4.96
Gasbjerg, L. S. 2018	HGC-Saline		1.5	580.5	1292	259.4	773.2	2.23	2.98
Hansen, K. B. 2012 (b)	HGC-Saline		1.5					2.40	4.70
Jørgensen, M. B. 2019	HGC-Saline		2			223.8	506.8		2.26
Meier, J. J. 2001	HGC-No Saline		2	855	2167	77.8	215	2.53	2.76
Meier, J. J. 2005	HGC-No Saline		2	545	1417	85.6	189.2	2.60	2.21
Meneilly, G. S. 1998	HGC-Saline	Young	2			233	925.5		3.97
		Young	4			233	1167		5.01
		Old	2			197.7	626.6		3.17
		Old	4			197.7	713.3		3.61
Nauck, M. 1989	HGC-Saline		1.3	1421	2773	178.7	706.7	1.95	3.95
Pilgaard, K. 2009	HGC-No Saline		4	4.1*	7	84.4	171.8	1.71	2.04
Rudovich, N. N. 2004 (c)	HGC-No Saline		2	5.2*	15.2	130.2	580.2	2.92	4.46
Rudovich, N. N. 2005 (d)	HGC-No Saline		2			171	1074		6.28
Schou, J. H. 2005	HGC-No Saline		4	2.82*	6.45	71.8	148.8	2.29	2.07
Thondam, S. K. 2017	HGC-Saline	Lean	2			94.8	205.3		2.17
		Obese	2			193	298.8		1.55
Vilsbøll, T. 2003 (e)	HGC-Saline		1.5	878.6	1358	56.3	111	1.55	1.97

Table S4: Hyperglycemic clamps with concomitant GIP infusion. a) GIP was infused at 4 pmol·kg^{-1}·min^{-1} for 15 min and then at 2 pmol·kg^{-1}·min^{-1} for 45 min; b) the AUC fold increase was reported in the manuscript (Table 2); c) ISR, which was expressed in pmol/min, has been divided by 70 kg body weight; d) values measured at t=60 min and t=90 min; e) mean values for the 7 mmol/L glucose step of the hyperglycemic clamp; *) studies reporting insulin secretion in pmol·kg^{-1}·min^{-1}.

Column headings of Table S4:
Reference: Reference to the study.
Protocol: HGC-Saline: hyperglycemic glucose clamp with saline infusion as control test; HCG-No Saline: hyperglycemic glucose clamp without saline infusion and a control period during the clamp; HI-HGC: hyperinsulinemic hyperglycemic clamp, with insulin infusion during a standard hyperglycemic clamp and saline infusion as control test.
Group: Study subgroup (e.g. GIP dose) when data are reported for subgroups.
GIP dose: GIP infusion dose (pmol·kg^{-1}·min^{-1}).
CTR ISR: Insulin secretion in the control test (saline infusion or clamp period, according to protocol). Insulin secretion is given in pmol·kg^{-1}·min^{-1} when calculated by deconvolution from C-peptide (starred data) or in pmol/L when only C-peptide is provided. Values are means (as AUC/time) during the reference period.
GIP ISR: Insulin secretion in the GIP infusion test (separate clamp or clamp period, according to protocol). Data are presented as for *CTR ISR*.
CTR INS: Insulin concentration in the control test (saline infusion or clamp period, according to protocol). Insulin concentration is given in pmol/L. Values are means (as AUC/time) during the reference period.
GIP INS: Insulin concentration in the GIP infusion test (separate clamp or clamp period, according to protocol). Data are presented as for *CTR INS*.
POT ISR: Potentiating effect of GIP on insulin secretion, calculated as (*GIP ISR*)/(*CTR ISR*).
POT INS: Potentiating effect of GIP on insulin concentration, calculated as (*GIP INS*)/(*CTR INS*).

4 Supplementary figures

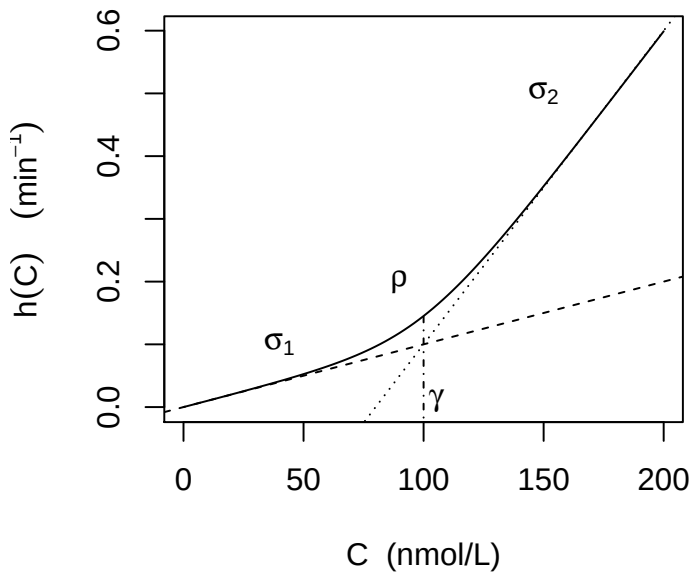

Figure S1: Function $h(C)$ used for exocytosis and refilling (Equation S.5). The scale of C, $h(C)$ and the parameters used in the plot are illustrative.

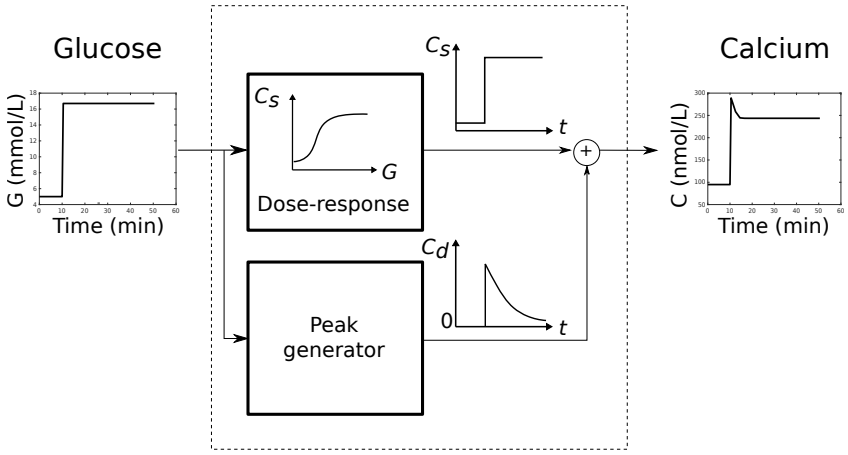

Figure S2: Scheme of the glucose-calcium model. The model predicts calcium from glucose based on the static dose-response (C_s, Equation S.11) and the addition of a calcium peak when glucose increases abruptly (C_d, Equations S.12- S.13).

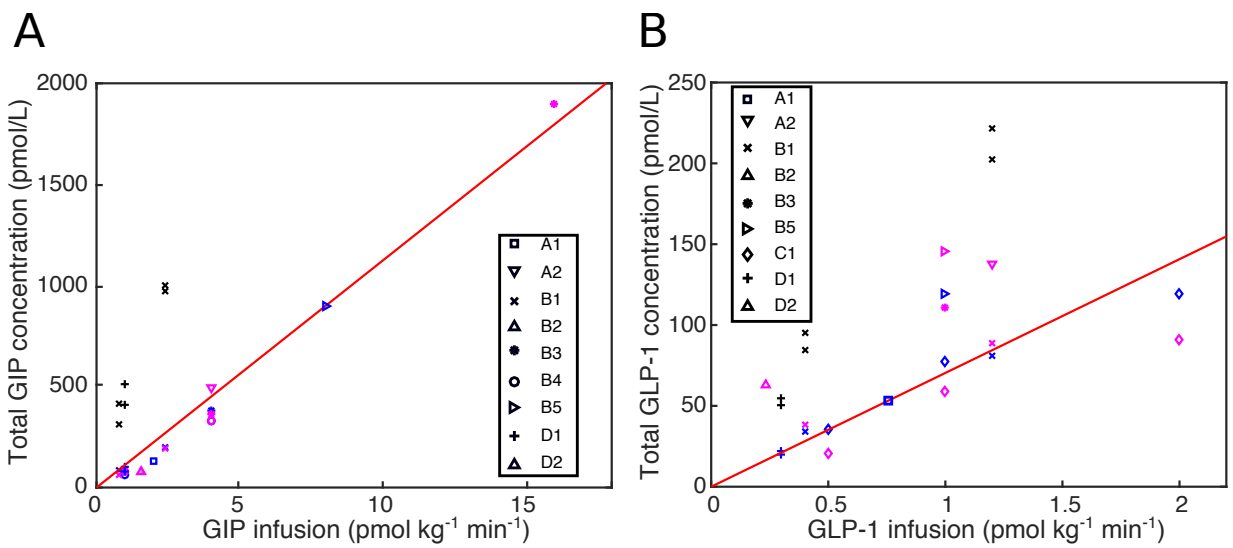

Figure S3: Relationships between GIP and GLP-1 infusion and average concentration in the studies considered in this work. As described in the Methods in the main text, the values in studies B1 and D1, which were obtained using an assay with very different characteristics, were rescaled. The black symbols show the values of the hormones concentrations before rescaling. The original values were 5 times greater for GIP and 2.5 times greater for GLP-1. In study B5, which reported only intact GIP, total GIP was extrapolated from the regression line (red line), given the dose. An analogous approach was used in study A1, in which only intact GLP-1 was available. The studies in NGT subjects are shown in blue and those in T2D subjects in purple.

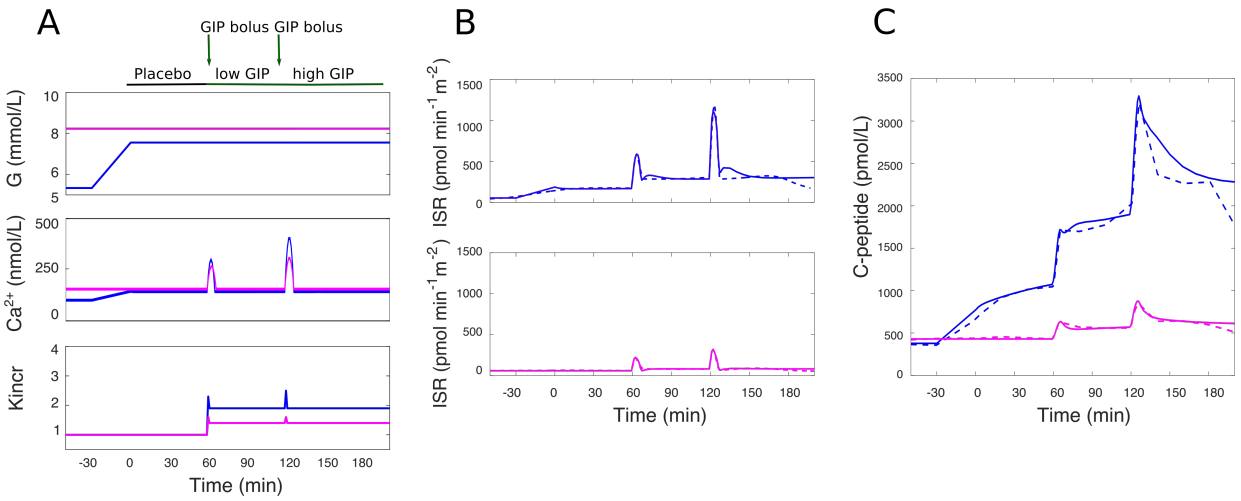

Figure S4: Simulation of Study B4, a hyperglycemic clamp with infusion of GIP at two doses in NGT (blue lines) and T2D (purple lines) subjects. A) Glucose (G) and Ca^{2+} concentrations and K_{incr}. With saline infusion, where $K_{incr} = 1$, the gradual increase with time in insulin secretion in NGT subjects is simulated by an increase in K_{glu}, which rises to 1.2 at the end of the test. The increase is absent in T2D subjects. B) Simulated (continuous lines) and C-peptide-derived insulin secretion (ISR) (dashed lines). C) Simulated (continuous lines) and measured C-peptide concentration (dashed lines). In correspondence to the GIP boluses, which cause a brisk peak in GIP concentration, both calcium and K_{incr} exhibit a spike, which contribute to the insulin secretion peak.

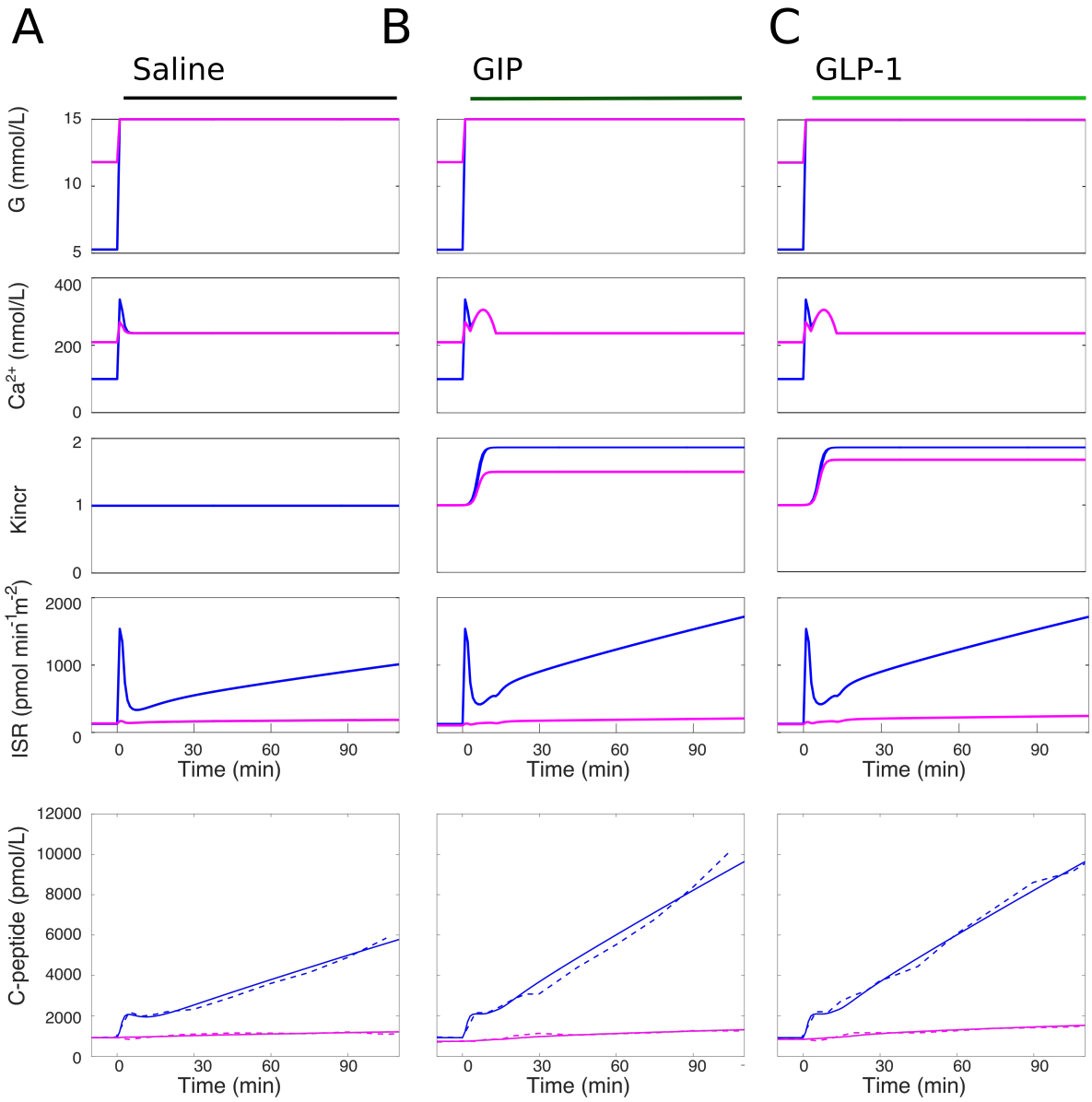

Figure S5: Simulation of Study B2, a hyperglycemic clamp with continuous infusion of saline (A), GIP (B) or GLP-1 (C) in NGT subjects (blue lines) or T2D subjects (purple lines). The panels show glucose (G) and Ca^{2+} concentrations, K_{incr}, insulin secretion (ISR) and simulated (continuous lines) and measured (dashed lines) C-peptide concentration. With saline infusion, where $K_{incr} = 1$, ramping insulin secretion is simulated by a gradual increase in K_{glu}, which rises to 2.8 at the end of the test in NGT subjects and to 1.4 in T2D subjects. It is hypothesized that the same K_{glu} increase underlies also the GIP and GLP-1 infusion tests, in which the greater increase in insulin secretion is explained by K_{incr}, determined empirically.

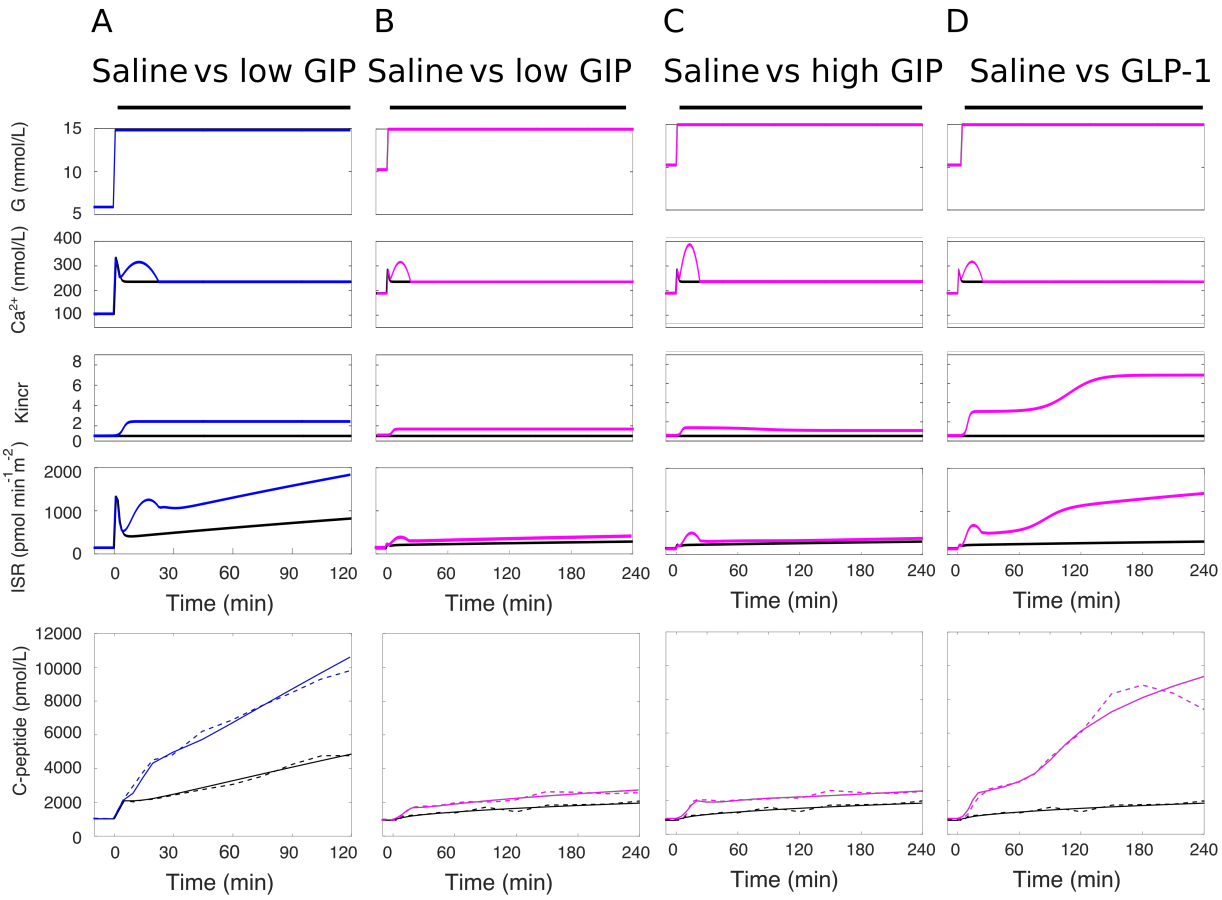

Figure S6: Simulation of Study B3, a hyperglycemic clamp with infusion of saline, GIP at low and high dose, and GLP-1, in NGT (blue lines, panel A) and T2D (purple lines, panels B-D) subjects. All panels show the saline (black lines) and incretin-stimulated (colored lines) results superimposed. The panels show glucose (G) and Ca^{2+} concentrations, K_{incr}, insulin secretion (ISR) and simulated (continuous lines) and measured (dashed lines) C-peptide concentration. With saline infusion, where $K_{incr} = 1$, ramping insulin secretion is simulated by a gradual increase in K_{glu}, which rises to 2.8 at the end of the test in NGT subjects and 1.4 in T2D subjects. It is hypothesized that the same K_{glu} increase underlies also the GIP and GLP-1 infusion tests, in which the greater increase in insulin secretion is explained by K_{incr}, determined empirically. K_{incr} in panels B and C is similar, despite the very different GIP doses (4 pmol·kg^{-1}·min^{-1}in panel B and 16 pmol·kg^{-1}·min^{-1} in panel C), indicating that the effect of GIP saturates. At the low GIP dose, K_{incr} in NGT subjects (panel A) was higher than in T2D subjects (panel B), but far lower than that reached during GLP-1 infusion in T2D subjects (panel D).

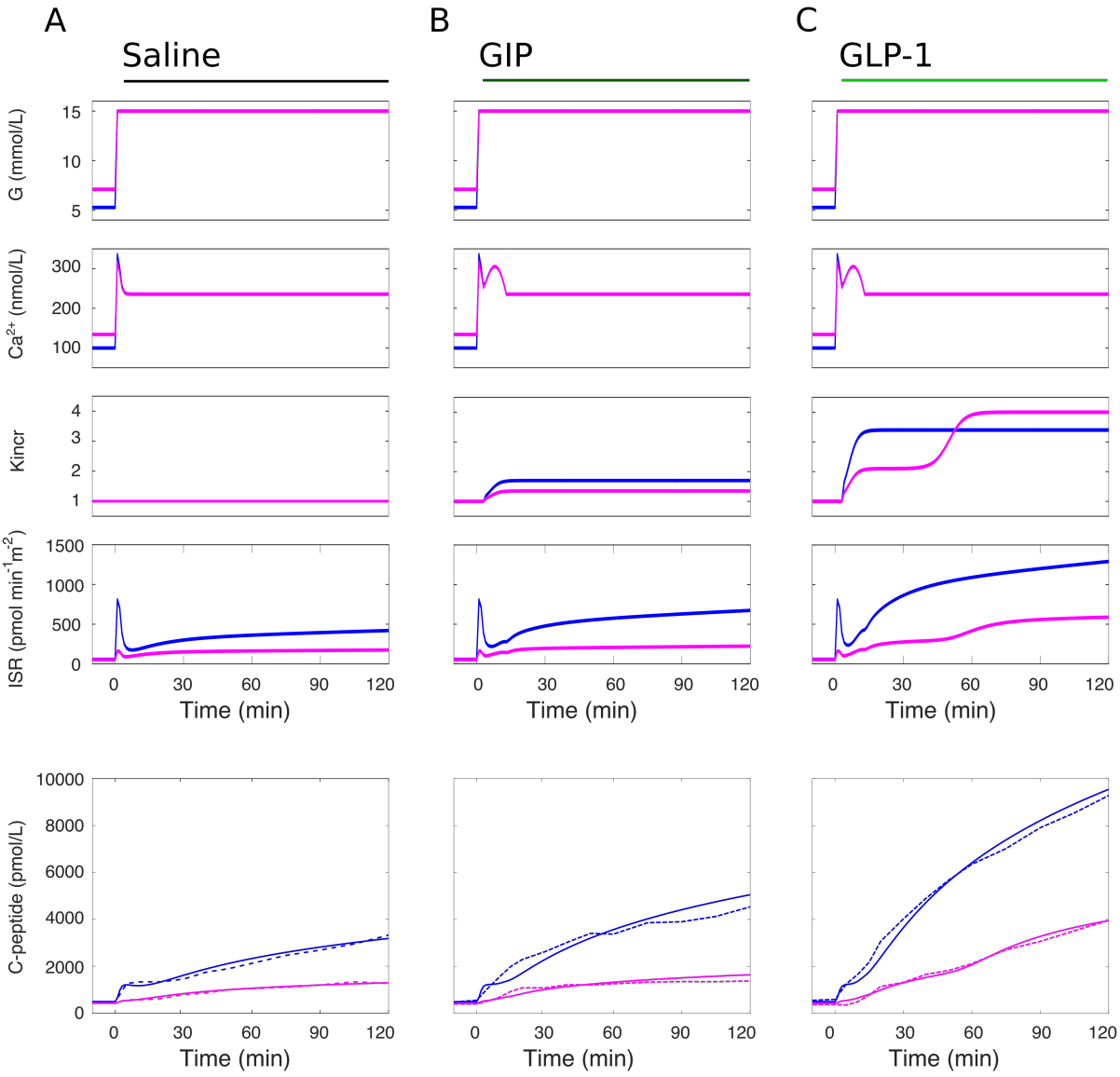

Figure S7: Simulation of Study B5, a hyperglycemic clamp with continuous infusion of saline (A), GIP (B) or GLP-1 (C) in NGT subjects (blue lines) or T2D subjects (purple lines) with chronic pancreatitis. The panels show glucose (G) and Ca^{2+} concentrations, K_{incr}, insulin secretion (ISR) and simulated (continuous lines) and measured (dashed lines) C-peptide concentration. With saline infusion, where $K_{incr} = 1$, ramping insulin secretion is simulated by a gradual increase in K_{glu}, which rises to 1.4 at the end of the test in NGT subjects and to 1.2 in T2D subjects. It is hypothesized that the same K_{glu} increase underlies also the GIP and GLP-1 infusion tests, in which the greater increase in insulin secretion is explained by K_{incr}, determined empirically

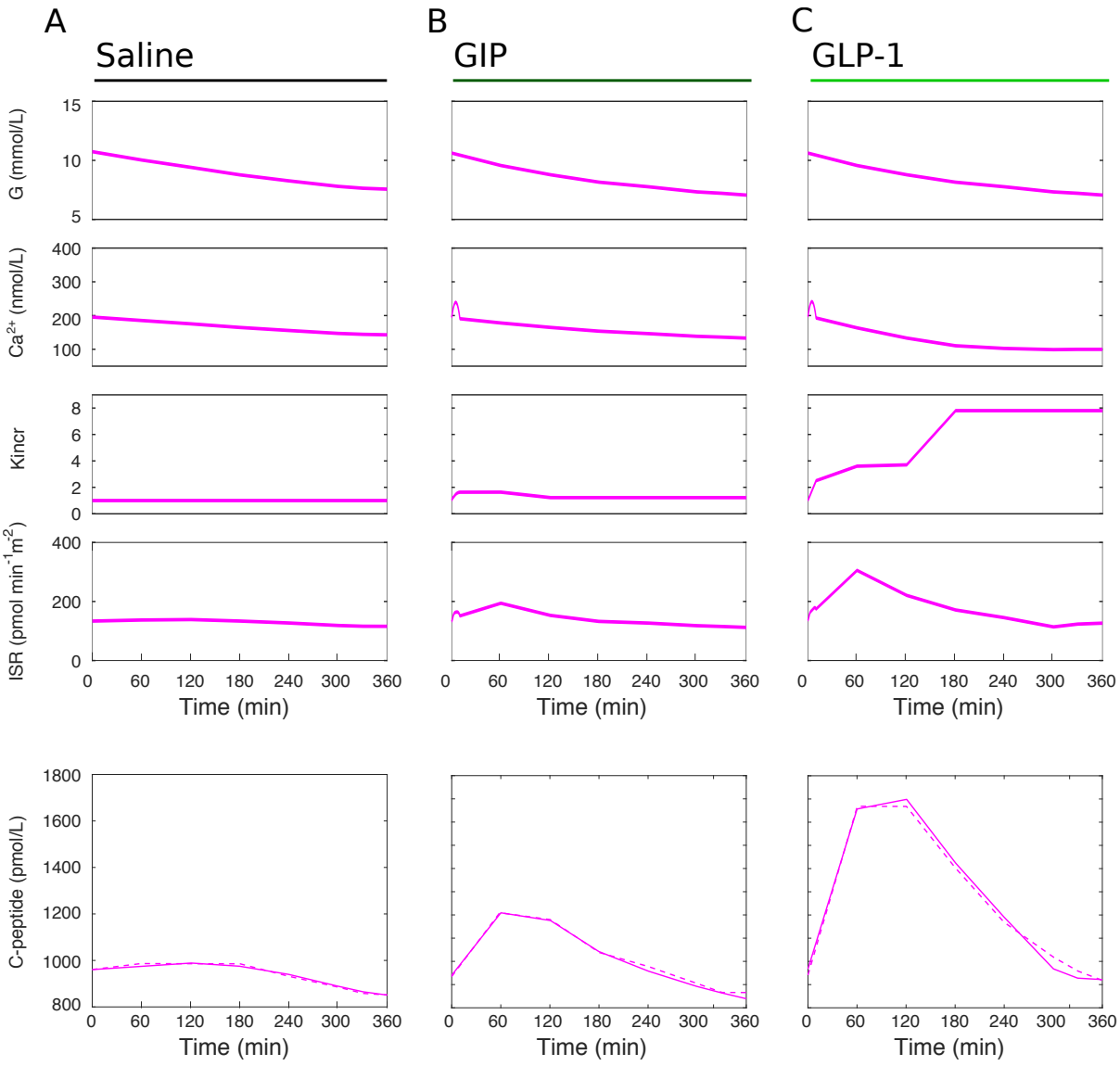

Figure S8: Simulation of Study A2, an infusion of saline (A), GIP (B) or GLP-1 (C) in T2D subjects, starting at basal glucose. With saline infusion, where $K_{incr} = 1$, the fall in insulin secretion with falling glucose is prevented by an increase in K_{glu}, which rises to 2.2 at the end of the test. It is hypothesized that the same K_{glu} increase underlies also the GIP and GLP-1 infusion tests, in which the greater increase in insulin secretion is explained by K_{incr}, determined empirically. With GIP infusion, the increase in K_{incr} is modest (1.3 on average) in spite of the high hormone levels, while with GLP-1 it is much greater (5.9 on average).

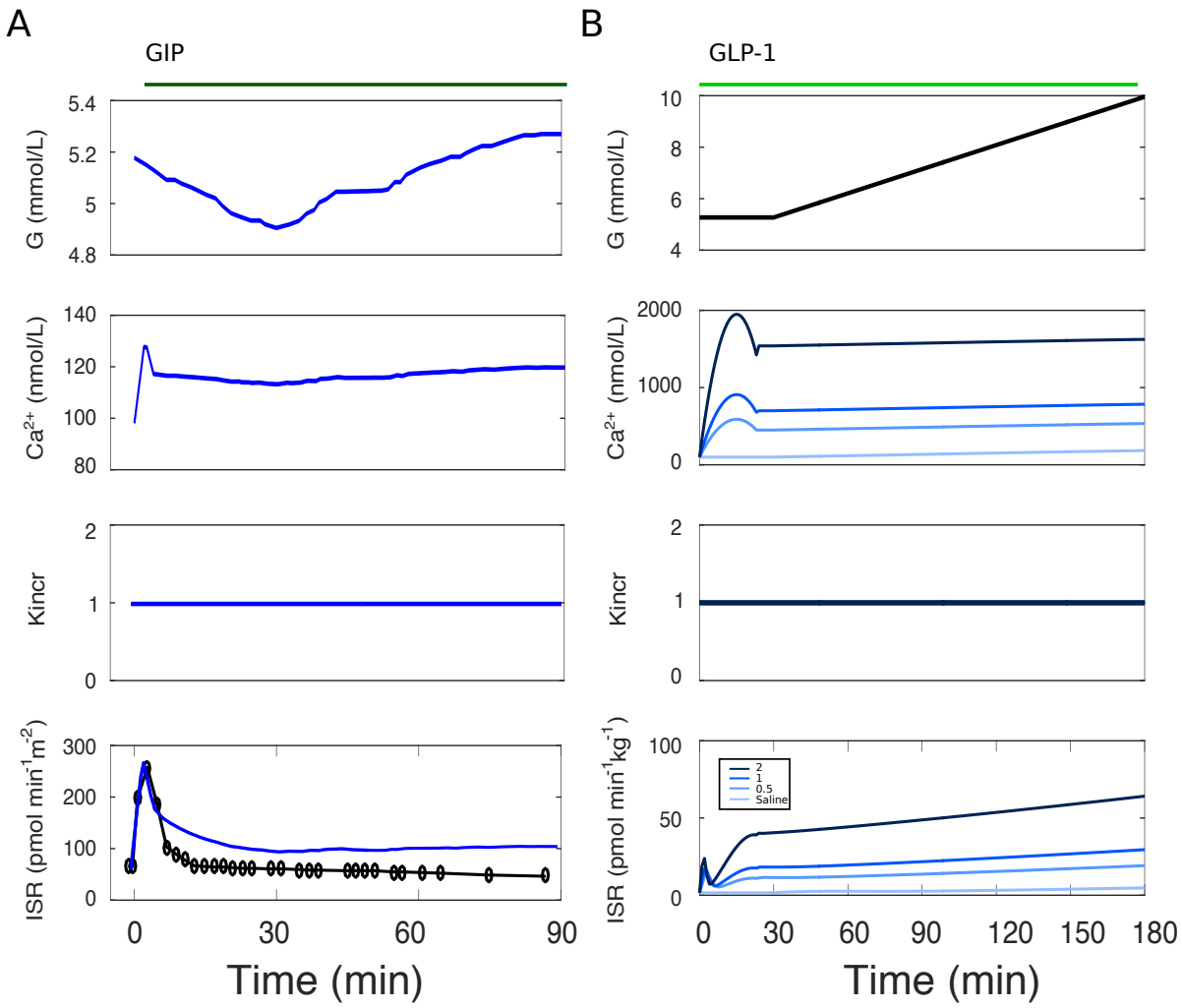

Figure S9: Simulation of the effects of sustained elevated calcium as a possible action of incretin hormones. The panels show glucose (G) and Ca^{2+} concentrations, K_{incr} and insulin secretion (ISR). In all simulations $K_{incr} = 1$. A) Protracted, rather than transient, calcium elevation in Study A1 (to $\sim$120 $nmol/L$ from a baseline of $\sim$100 $nmol/L$) would produce a sustained increase in insulin secretion, in disagreement with the data (black line in the lowest panel). B) In the graded glucose infusion study with GLP-1 infusion (Study C1), the observed strong increase in insulin secretion with high GLP-1 doses could be explained by an effect on calcium alone. However, this hypothesis would require highly supraphysiological calcium levels.

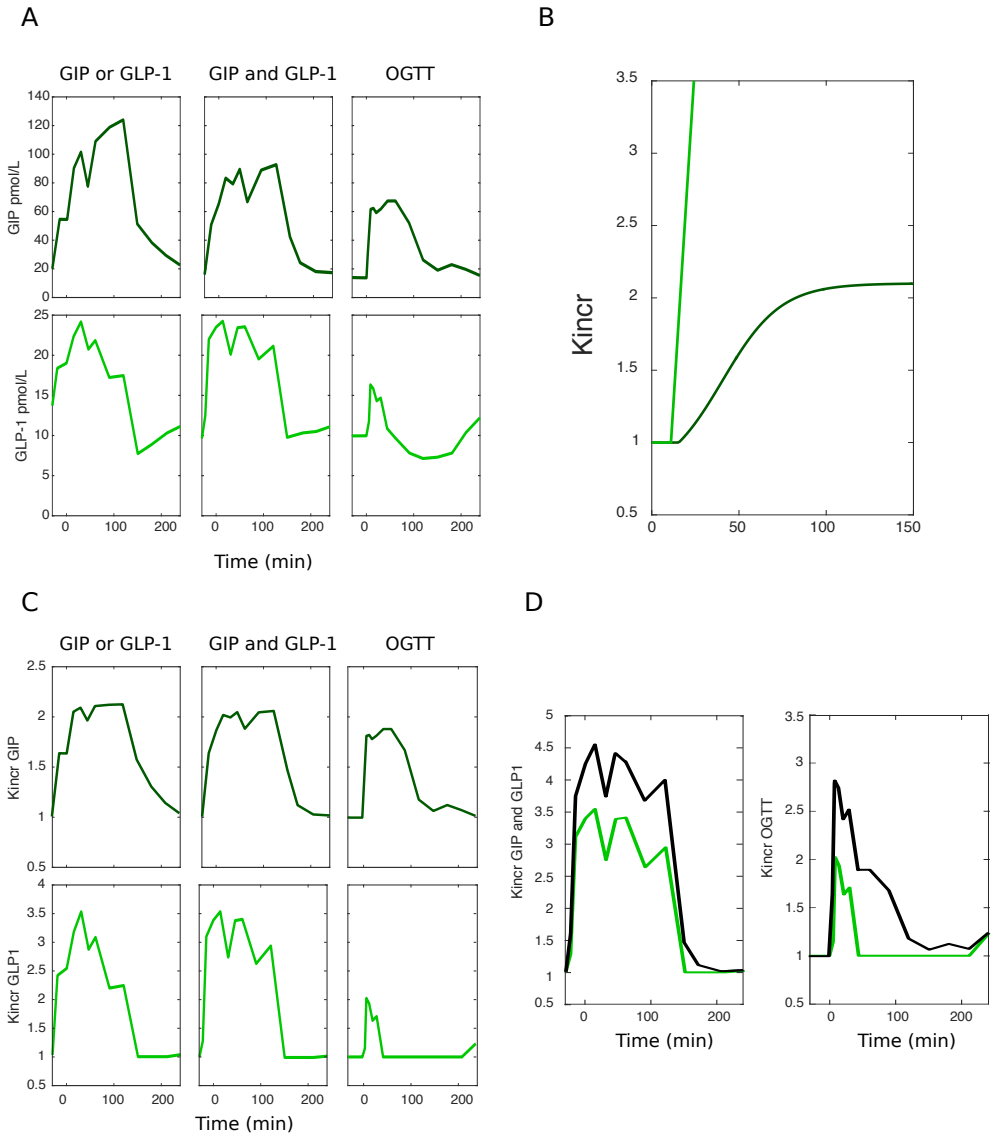

Figure S10: Calculation of K_{incr} from GIP and GLP-1 measured concentrations in the tests of Study D1, reported in Figure 6 of the main text. A) Total GIP (dark green) and GLP-1 (light green) concentrations measured in the tests with separate GIP or GLP-1 infusions (left), GIP and GLP-1 co-infusion (middle) and OGTT (right). B) Relationships between K_{incr} and GIP (Equation S.16, dark green) and GLP-1 (Equation S.15, light green) concentrations for this study, adapted from Figure 5 of the main text. C) K_{incr} calculated from GIP and GLP-1 concentrations of panel A, using the relationships of panel B. The K_{incr} values of the left panel column were used in the simulations reported in Figures 6B an 6C of the main text. D) K_{incr} calculated in the test with GIP and GLP-1 co-infusion (left panel, black line) and in the OGTT (right panel, black line), assuming an additive effect (Equation S.17). The green lines in both panels represent the contribution to K_{incr} due to GLP-1. The difference between the black and the green lines represent the contribution to K_{incr} due to GIP. The K_{incr} values plotted in black were used in the simulation reported in Figures 6D and 6E of the main text.

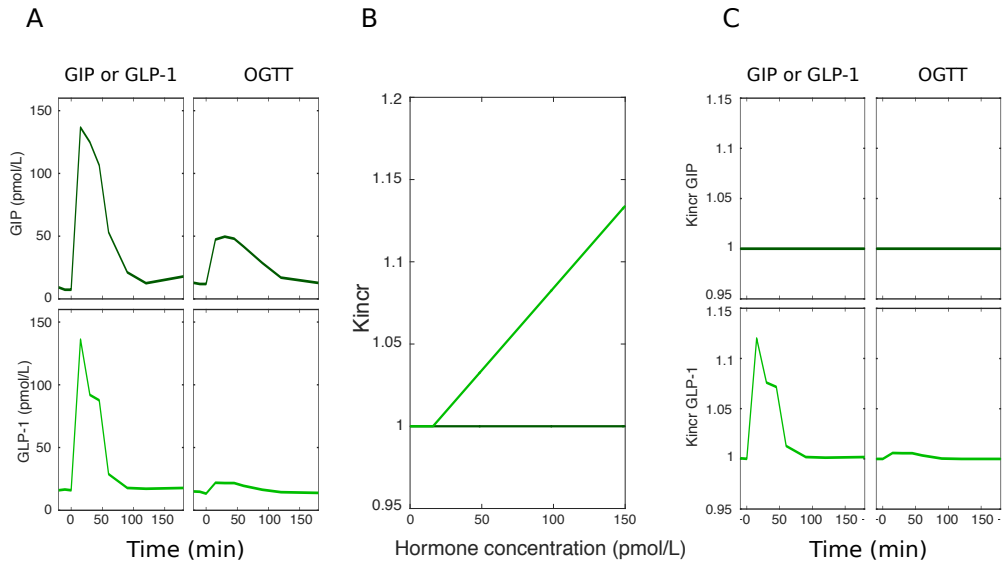

Figure S11: Calculation of K_{incr} from GIP and GLP-1 measured concentrations in Study D2, reported in Figure 7 of the main text. A) Total GIP (dark green) and GLP-1 (light green) concentrations measured in the tests with separate GIP or GLP-1 infusion (left), and OGTT (right). B) Relationships between K_{incr} and GIP (Equation S.16, dark green) and GLP-1 (Equation S.15, light green) concentrations for this study. C) K_{incr} calculated from GIP and GLP-1 concentrations of panel A, using the relationships of panel B. These K_{incr} values were used in the simulations reported in Figures 7B (GIP infusion), 7C (GLP-1 infusion) and 7D (OGTT) of the main text.

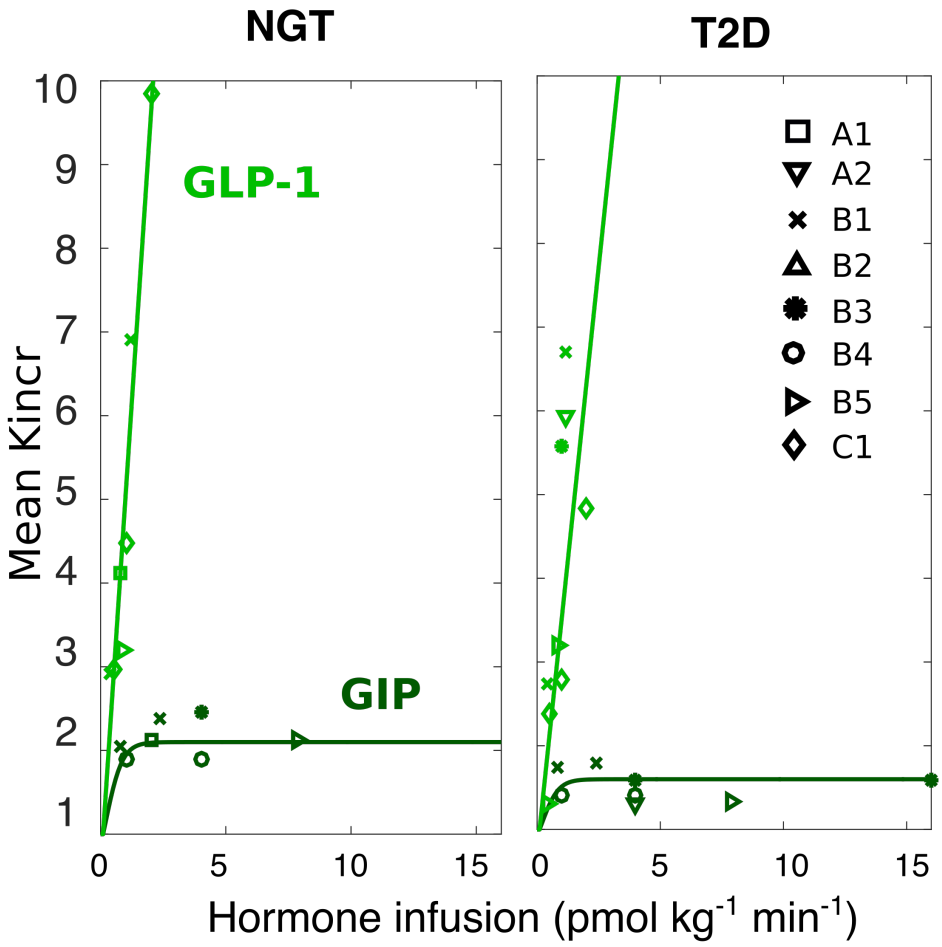

Figure S12: Relationships between K_{incr} and GIP (dark green lines) or GLP-1 (light green lines) infusion in the studies with incretin hormone infusion, represented by the different markers. This figure reproduces the results of Figure 5 of the main text, using in the abscissa the hormone infusion instead of the concentration.

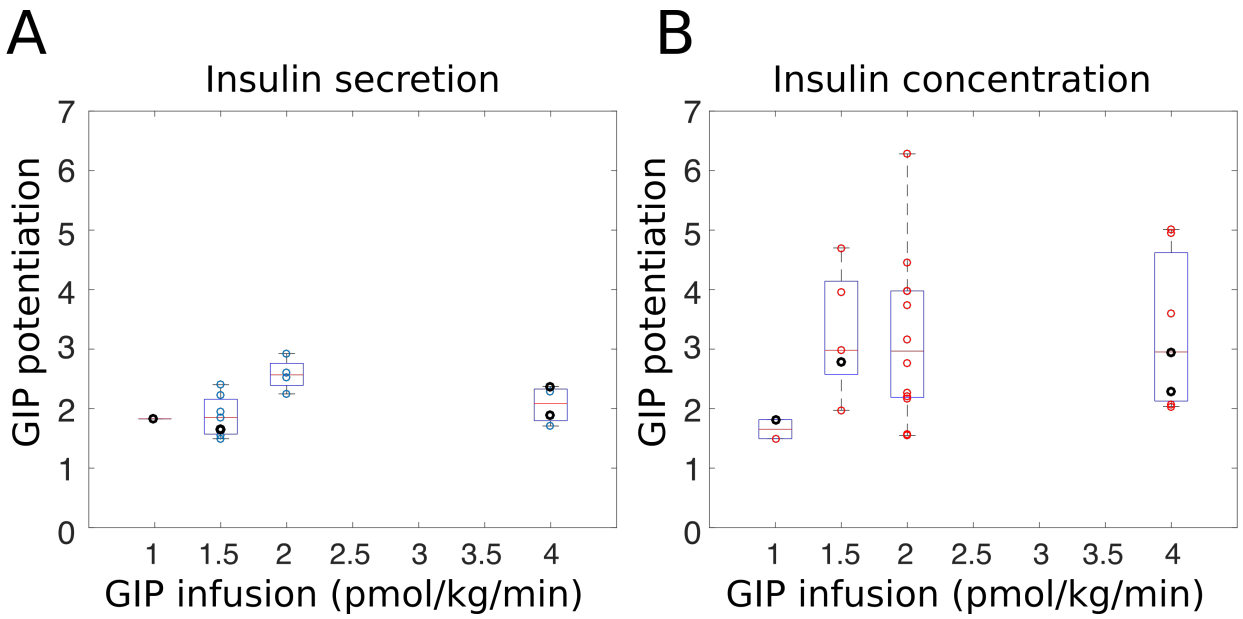

Figure S13: Potentiating effect of GIP calculated from the studies reported in Table S4 from insulin secretion (A) or insulin concentration (B).The study by Nauck et al., 1989, employing a 1.3 pmol·kg^{-1}·min^{-1} infusion, is represented in the boxplot at 1.5 pmol·kg^{-1}·min^{-1}. The black dots show the potentiating effect of GIP calculated from three of the studies simulated with the model (studies B2, B3 and B4).

References

Asmar, M., Simonsen, L., Madsbad, S., Stallknecht, B., Holst, J. J., & Bulow, J. (2010, September). Glucose-dependent insulinotropic polypeptide may enhance fatty acid re-esterification in subcutaneous abdominal adipose tissue in lean humans. *Diabetes*, *59*(9), 2160–2163.

Christensen, M., Vedtofte, L., Holst, J. J., Vilsbøll, T., & Knop, F. K. (2011, December). Glucose-dependent insulinotropic polypeptide: a bifunctional glucose-dependent regulator of glucagon and insulin secretion in humans. *Diabetes*, *60*(12), 3103–3109.

Dirksen, C., Bojsen-Møller, K. N., Jørgensen, N. B., Jacobsen, S. H., Kristiansen, V. B., Naver, L. S., ... Madsbad, S. (2013, December). Exaggerated release and preserved insulinotropic action of glucagon-like peptide-1 underlie insulin hypersecretion in glucose-tolerant individuals after Roux-en-Y gastric bypass. *Diabetologia*, *56*(12), 2679–2687.

Elahi, D., McAloon-Dyke, M., Fukagawa, N. K., Meneilly, G. S., Sclater, A. L., Minaker, K. L., ... Andersen, D. K. (1994, April). The insulinotropic actions of glucose-dependent insulinotropic polypeptide (GIP) and glucagon-like peptide-1 (7-37) in normal and diabetic subjects. *Regul Pept*, *51*(1), 63–74.

Gasbjerg, L. S., Christensen, M. B., Hartmann, B., Lanng, A. R., Sparre-Ulrich, A. H., Gabe, M. B. N., ... Knop, F. K. (2018, February). GIP(3-30)NH2 is an efficacious GIP receptor antagonist in humans: a randomised, double-blinded, placebo-controlled, crossover study. *Diabetologia*, *61*(2), 413–423.

Grespan, E., Giorgino, T., Arslanian, S., Natali, A., Ferrannini, E., & Mari, A. (2018, March). Defective amplifying pathway of β-cell secretory response to glucose in type 2 diabetes: integrated modeling of in vitro and in vivo evidence. *Diabetes*, *67*(3), 496–506.

Hansen, K. B., Vilsbøll, T., Bagger, J. I., Holst, J. J., & Knop, F. K. (2012, April). Impaired incretin-induced amplification of insulin secretion after glucose homeostatic dysregulation in healthy subjects. *J Clin Endocrinol Metab*, *97*(4), 1363–1370.

Henquin, J.-C., Nenquin, M., Stiernet, P., & Ahren, B. (2006, February). In vivo and in vitro glucose-induced biphasic insulin secretion in the mouse pattern and role of cytoplasmic Ca^{2+} and amplification signals in β-cells. *Diabetes*, *55*(2), 441-451.

Jørgensen, M. B., Idorn, T., Rydahl, C., Hansen, H. P., Bressendorff, I., Brandi, L., ... Feldt-Rasmussen, B. (2019, October). Effect of the incretin hormones on the endocrine pancreas in end-stage renal disease. *J Clin Endocrinol Metab*, *In press*. doi: https://doi.org/10.1210/clinem/dgz048

Mari, A., Tura, A., Gastaldelli, A., & Ferrannini, E. (2002, February). Assessing insulin secretion by modeling in multiple-meal tests: role of potentiation. *Diabetes*, *51*(suppl 1), S221–226.

Meier, J. J., Gallwitz, B., Askenas, M., Vollmer, K., Deacon, C. F., Holst, J. J., ... Nauck, M. A. (2005, September). Secretion of incretin hormones and the insulinotropic effect of gastric inhibitory polypeptide in women with a history of gestational diabetes. *Diabetologia*, *48*(9), 1872–1881.

Meier, J. J., Hucking, K., Holst, J. J., Deacon, C. F., Schmiegel, W. H., & Nauck, M. A. (2001, November). Reduced insulinotropic effect of gastric inhibitory polypeptide in first-degree relatives of patients with type 2 diabetes. *Diabetes*, *50*(11), 2497–2504.

Meneilly, G. S. (1998, August). The effect of age and glycemic level on the response of the β-cell to glucose-dependent insulinotropic polypeptide and peripheral tissue sensitivity to endogenously released insulin. *J Clin Endocrinol Metab*, *83*(8), 2925–2932.

Nauck, M., Schmidt, W. E., Ebert, R., Strietzel, J., Cantor, P., Hoffmann, G., & Creutzfeldt, W. (1989, September). Insulinotropic properties of synthetic human gastric inhibitory polypeptide in man: interactions with glucose, phenylalanine, and cholecystokinin-8. *J Clin Endocrinol Metab*, *69*(3), 654–662.

Nauck, M. A., Bartels, E., Ørskov, C., Ebert, R., & Creutzfeldt, W. (1993, April). Additive insulinotropic effects of exogenous synthetic human gastric inhibitory polypeptide and glucagon-like peptide-1-(7-36) amide infused at near-physiological insulinotropic hormone and glucose concentrations. *J Clin Endocrinol Metab*, *76*, 912–917.

Pilgaard, K., Jensen, C. B., Schou, J. H., Lyssenko, V., Wegner, L., Brøns, C., ... Vaag, A. A. (2009, July). The T allele of rs7903146 TCF7l2 is associated with impaired insulinotropic action of incretin hormones, reduced 24 h profiles of plasma insulin and glucagon, and increased hepatic glucose production in young healthy men. *Diabetologia*, *52*(7), 1298–1307.

Rudovich, N. N., Dick, D., Moehlig, M., Otto, B., Spranger, J., Rochlitz, H., ... Pfeiffer, A. (2005, April). Ghrelin is not suppressed in hyperglycemic clamps by gastric inhibitory polypeptide and arginine. *Regul Pept*, *127*(1-3), 95–99.

Rudovich, N. N., Rochlitz, H. J., & Pfeiffer, A. F. (2004, September). Reduced hepatic insulin extraction in response to gastric inhibitory polypeptide compensates for reduced insulin secretion in normal-weight and normal glucose

tolerant first-degree relatives of type 2 diabetic patients. *Diabetes*, *53*(9), 2359–2365.

Schou, J. H., Pilgaard, K., Vilsbøll, T., Jensen, C. B., Deacon, C. F., Holst, J. J., … Vaag, A. A. (2005, August). Normal secretion and action of the gut incretin hormones glucagon-like peptide-1 and glucose-dependent insulinotropic polypeptide in young men with low birth weight. *J Clin Endocrinol Metab*, *90*(8), 4912–4919.

Thondam, S. K., Daousi, C., Wilding, J. P. H., Holst, J. J., Ameen, G. I., Yang, C., … Cuthbertson, D. J. (2017, March). Glucose-dependent insulinotropic polypeptide promotes lipid deposition in subcutaneous adipocytes in obese type 2 diabetes patients: a maladaptive response. *Am J Physiol Endocrinol Metab*, *312*(3), E224–E233.

Vilsbøll, T., Krarup, T., Madsbad, S., & Holst, J. J. (2003, July). Both GLP-1 and GIP are insulinotropic at basal and postprandial glucose levels and contribute nearly equally to the incretin effect of a meal in healthy subjects. *Regul Pept*, *114*, 115–121.